Gramlich, V. & Meier, W. M. (1971). *Z. Kristallogr.* **133**, 134–149.
Hawthorne, F. C. (1978). *Acta Cryst.* A**34**, 139–140.
Ilyukhin, V. V., Nikitin, A. V. & Belov, N. V. (1966). *Dokl. Akad. Nauk SSSR*, **171**, 1325–1328 [Engl. trans. (1967). *Sov. Phys. Dokl.* **11**, 1035–1037].
International Tables for X-ray Crystallography (1974). Vol. IV. Birmingham: Kynoch Press.
Joubert-Bettan, C. A., Lachenal, R., Bertaut, E. F. & Parthe, E. (1969). *J. Solid State Chem.* **1**, 1–5.
Marumo, F., Isobe, M., Saito, Y., Yagi, T. & Akimoto, S. (1974). *Acta Cryst.* B**30**, 1904–1906.
Meier, W. M. & Villiger, H. (1969). *Z. Kristallogr.* **129**, 411–423.
O'Keeffe, M. & Hyde, B. G. (1976). *Acta Cryst.* B**32**, 2923–2936.
O'Keeffe, M. & Hyde, B. G. (1978). *Acta Cryst.* B**34**, 3519–3528.
Shannon, R. D. (1976). *Acta Cryst.* A**32**, 751–767.
Shannon, R. D. (1979). *Phys. Chem. Miner.* **4**, 139–148.
Shannon, R. D. & Berzins, T. (1979). *Mater. Res. Bull.* **14**, 361–367.
Solid Electrolytes (1978). Edited by P. Hagenmuller & W. van Gool. New York: Academic Press.
Strukturbericht 1913–1928 (1931). Vol. 1, pp. 128–129. Leipzig: Akademische Verlagsgesellschaft.
Swanson, H. E. & Fuyat, R. K. (1953). *Natl Bur. Stand. (US) Circ.* **593**, Vol. II, 25–26.
Takeuchi, Y. & Kudoh, Y. (1977). *Z. Kristallogr.* **146**, 281–292.
Tillmanns, E. & Baur, W. H. (1970). *Acta Cryst.* B**26**, 1645–1654.
Tillmanns, E., Gebert, W. & Baur, W. H. (1973). *J. Solid State Chem.* **7**, 69–84.
Tranqui, D., Capponi, J. J., Joubert, J. C., Shannon, R. D. & Johnson, C. K. (1979). Int. Conf. Fast Ion Transport in Solids – Electrolytes and Electrodes, Lake Geneva, Program and Abstracts, PA-25.

Acta Cryst. (1981). B**37**, 1491–1496

Structural Aspects of the Hexagonal to Orthorhombic Transition in Stoichiometric $BaVS_3$

By M. Ghedira,* J. Chenavas, F. Sayetat and M. Marezio
Laboratoire de Cristallographie, CNRS, 166*X*, 38042 *Grenoble CEDEX, France*
and O. Massenet and J. Mercier
Groupe des Transitions de Phases, 166*X*, 38042 *Grenoble CEDEX, France*

(*Received* 18 *February* 1980; *accepted* 27 *January* 1981)

Abstract

The crystal structure of stoichiometric $BaVS_3$ has been refined at room temperature from single-crystal X-ray data. This compound is hexagonal, space group $P6_3/mmc$ with two molecules per unit cell of dimensions $a = 6{\cdot}7283\ (5)$ and $c = 5{\cdot}6263\ (5)$ Å. The structure has been refined to a final R value of 1·1% for 216 independent reflections. The sulfur and the barium atoms form a slightly distorted hexagonal close-packed network with the vanadium atoms occupying one quarter of the octahedral sites, namely those formed only by sulfur atoms. These vanadium-occupied sulfur octahedra share faces and form infinite chains parallel to the c hexagonal axis. This arrangement makes $BaVS_3$ a 1*D* compound as far as the vanadium atoms are concerned. The average V—S distance is 2·385 (1) Å. The barium atoms are surrounded by 12-sulfur polyhedra, the average Ba—S distance being 3·396 (1) Å. These results are in good agreement with those previously published by Gardner, Vlasse & Wold [*Acta Cryst.* (1969), B**25**, 781–787]. The thermal vibrations of the vanadium atoms are strongly anisotropic. The r.m.s. value in the basal plane is 0·163 (1) Å, whereas that along the c axis is 0·106 (1) Å. This seems to indicate that already in the hexagonal phase the vanadium atoms zig-zag along the c axis, which can be considered as a dynamical distortion of the vanadium sublattice. Single-crystal X-ray data at low temperature show that stoichiometric $BaVS_3$ undergoes a crystallographic phase transition at about 250 K. Since the crystal symmetry becomes orthorhombic, twin formation is observed at the transition. The twinning is by pseudomerohedry. Precession photographs of twin crystals have been fully indexed on an orthorhombic cell of dimensions $a_O \simeq a_H$, $b_O \simeq \sqrt{3}a_H$ and $c_O \simeq c_H$. The possible space

---

* Permanent address: Faculté des Sciences de Monastir, Monastir, Tunisie.

0567-7408/81/081491-06$01.00

groups are either $Cmc2_1$ or $C222_1$ with four molecules per unit cell. In either space group, the distortion of the vanadium sublattice consists of a static zig-zag of the vanadium atoms along the *c* axis. Therefore, the crystallographic transition can be considered as a dynamical to static distortion of the vanadium sublattice.

Introduction

As determined by Gardner, Vlasse & Wold (1969), the structure of $BaVS_3$ is hexagonal and contains a slightly distorted hexagonal-close-packed network which is composed of barium and sulfur atoms. The vanadium atoms occupy one quarter of the octahedral sites of this network, namely those which are made exclusively of sulfur atoms. These occupied octahedra share faces and form infinite chains along the *c* hexagonal axis. The chains are isolated from each other, which makes $BaVS_3$ a 1*D* compound as far as the vanadium atoms are concerned. Fig. 1 shows a projection of the structure along the *c* axis. One can readily see the hexagonal close-packed layers parallel to the basal *ab* plane and the isolated chains of vanadium-occupied octahedra.

The above authors reported that the resistivity of $BaVS_3$ decreased with decreasing temperature until 130 K indicating a metallic behavior, whereas below 130 K the resistivity increased sharply with decreasing temperature, indicating a semiconductor behavior. They also reported that at about 185 K $BaVS_3$ underwent a crystallographic distortion, indexed the X-ray powder pattern taken at 77 K on an orthorhombic cell, and stated that this crystallographic distortion was associated with the change of slope in the resistivity curve.

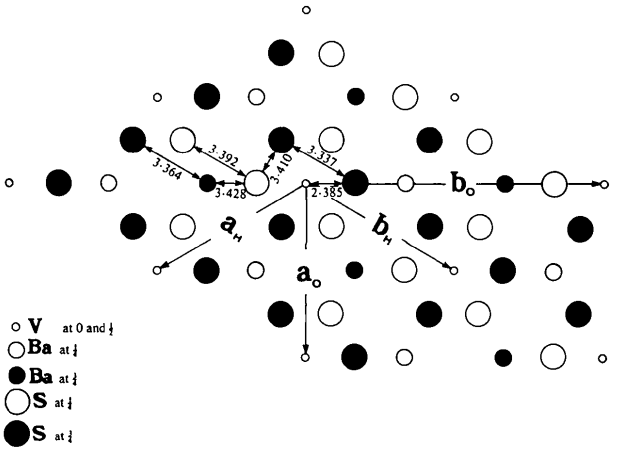

Fig. 1. A projection of the hexagonal structure of $BaVS_3$ on the *ab* plane. The most important distances (Å) in the hexagonal structure and the directions of the *a* and *b* orthorhombic axes are indicated.

Takano, Kosugi, Nakanishi, Shimada, Wada & Koizumi (1977) established from electrical resistivity, magnetic susceptibility, Mössbauer effect and X-ray diffraction measurements, performed on powder samples of $BaVS_3$ between 4 and 300 K, that the crystallographic transition began to occur at 258 K, while the sharp increase in the electrical resistivity occurred at about 70 K. This latter transition was accompanied by a sharp peak in the magnetic susceptibility, which suggested an antiferromagnetic ordering. The antiferromagnetic phase was confirmed by Mössbauer spectra performed on a powder sample of $BaVS_3$ containing 1% of ^{57}Fe. These authors concluded that the electrical transition was associated with the magnetic one; however they did not find any correlation between the electrical and the crystallographic transitions.

At about the same time Massenet *et al.* (1978) reported the results of electrical, magnetic, Mössbauer, EPR and X-ray diffraction studies performed on powder samples of $BaVS_3$ with different sulfur stoichiometry. Their results were in agreement with those of Takano *et al.* (1977). Furthermore, they showed that the physical properties and the transition temperatures were sensitive to the sulfur stoichiometry, which partly reconciled the results of Gardner *et al.* (1969) with those of Takano *et al.* (1977). However, Massenet *et al.* (1978) clearly established that there was no correlation between the crystallographic transition occurring at about 258 K and the 70 K transition. The most important results obtained by Massenet *et al.* (1978) were on samples with low sulfur content. These compounds showed a moderately Curie–Weiss behavior down to 25 K and ferromagnetic ordering below 16 K. For these non-stoichiometric samples the crystallographic transition occurred at about 150 K and the orthorhombic lattice distortion at 11 K was four times smaller than that of a stoichiometric sample at the same temperature.

This paper reports the structural refinement of stoichiometric $BaVS_3$ based on X-ray single-crystal data taken at room temperature, together with single-crystal data of the orthorhombic phase. A model is proposed for the transition from the hexagonal to the orthorhombic phase.

Experimental

The preparations of the powder and single-crystal samples used in these experiments have been described elsewhere (Massenet *et al.*, 1979). At room temperature the lattice parameters were determined with a powder Guinier camera equipped with monochromatic Fe *Kα* radiation. They were found to be a = 6·7283 (5), c = 5·6263 (5) Å. Precession photographs taken with Mo *Kα* radiation confirmed the $P6_3/mmc$

space group, the only systematic absences being *hhl* for $l = 2n + 1$. The room-temperature structural refinement was based on X-ray intensity measurements taken with an automatic Philips diffractometer using a graphite monochromator and Ag $K\alpha$ radiation. The sample was a sphere of 0·24 mm diameter. The integrated intensities were obtained by the use of ω scans, while the background was collected at ±0·6° off the peak maximum. All the reflections included in the interval $3 < 2\theta < 30°$ were measured; 216 independent reflections well above background were used in the refinement. Lorentz, polarization and absorption corrections were applied in order to convert the integrated intensities into structure factors. The structural refinement was carried out with the *LINEX* program (unpublished least-squares refinement program) together with the *f* curves for neutral atoms given by Cromer & Waber (1965). The real and imaginary anomalous-correction coefficients for barium and vanadium were those given by Cromer & Liberman (1970). The positional and thermal parameters of $BaVS_3$ given by Gardner *et al.* (1969) were used as the starting values. All reflections were given unit weight. The final positional and anisotropic thermal parameters are listed in Table 1. They correspond to a conventional R factor of 1·1%.* These values together with the lattice parameters previously given were used in order to calculate the interatomic distances and angles with their standard deviations. These values are reported in Table 2.

Table 1. *Positional and thermal* ($\times 10^4$ Å^2) *parameters at room temperature*

	Ba	V	S
x	$\frac{1}{3}$	0	0·16531 (8)
y	$\frac{2}{3}$	0	0·33062
z	$\frac{3}{4}$	0	$\frac{1}{4}$
U_{11}	100·6 (6)	266 (3)	105 (1)
U_{22}	100·6	266	77 (1)
U_{33}	132·0 (9)	113 (3)	138 (2)
U_{12}	50·3	133	38
U_{13}	0	0	0
U_{23}	0	0	0

By symmetry: $U_{13} = U_{23} = 0$; $U_{12} = \frac{1}{2}U_{22}$.

Table 2. *Interatomic distances* (Å) *and angles* (°) *at room temperature*

Barium polyhedron			
Ba–S	3·3642 (9)		
Ba–S	3·4275 (6)	S–Ba–S	59·31 (1)
S–S	3·392 (1)	S–Ba–S	60·26 (2)
S–S	3·410 (1)		
Vanadium octahedron			
V–S	2·3853 (8)	S–V–S	88·76 (1)
S–S	3·337 (1)	S–V–S	91·24 (1)
S–S	3·410 (1)		
Cation–cation separations			
V–V	2·8132 (3)	across the shared face	
V–V	6·7283 (5)	between adjacent chains	
V–Ba	4·1314 (4)		
Ba–Ba	4·7962 (5)		

Results

As can be seen from Table 2 our structural refinement yielded interatomic distances and angles which are in good qualitative agreement with the values reported by Gardner *et al.* (1969). The only improvement is in the standard deviations; in general our values are smaller by a factor of three.

The octahedra around the vanadium atoms have $\bar{3}m$ point symmetry and the six V–S distances are all 2·3853 ± 0·0008 Å. These octahedra are elongated along the *c* axis as the six S–S distances in the hexagonal-close-packed layers are 3·337 ± 0·001 Å while the six distances between two different layers are 3·410 ± 0·001 Å. This distortion allows a reasonable V–V distance (2·8132 ± 0·0003 Å) across the shared face.

The 12-sulfur polyhedra around the barium atoms are also elongated along the *c* axis; however, their elongation is smaller than that of the octahedra around the vanadium atoms. The S–S separation in the hexagonal layers is 3·392 ± 0·001 Å whereas that between layers is 3·410 ± 0·001 Å. Consequently the six Ba–S distances (3·364 Å) in the hexagonal layers are smaller than the six (3·428 Å) between layers.

The vibrations of the barium atoms are only slightly anisotropic as the three principal axes of the thermal ellipsoid are almost the same [0·115 (1) as against 0·100 (1) Å], with the longest one along the *c* axis. In contrast, the thermal vibrations of the vanadium and sulfur atoms are anisotropic. The thermal ellipsoids of the vanadium atoms are largely contracted along the *c* axis. The principal axes in the basal *ab* plane are 0·163 (1) Å, whereas that along the *c* axis is 0·106 (1) Å. This seems to indicate that the V–V separation along the *c* axis is too short for a sulfide and in order to make it longer the vanadium atoms vibrate in such a way that at any given time they actually zig-zag along the *c* axis. The anisotropy of the thermal vibrations of the sulfur atoms seems to be correlated to that of the vanadium atoms. For the sulfur atom at $x \simeq 0{\cdot}16$, $y \simeq 0{\cdot}32$ and $z = \frac{1}{4}$ (see Fig. 1) the smallest principal axis of the thermal ellipsoid [0·088 (1) Å] forms an angle of 90° with the a_H axis and one of 30° with the b_H axis, while the largest principal axes

---

* Lists of structure factors have been deposited with the British Library Lending Division as Supplementary Publication No. SUP 35946 (2 pp.). Copies may be obtained through The Executive Secretary, International Union of Crystallography, 5 Abbey Square, Chester CH1 2HU, England.

[0·102 (1) and 0·118 (1) Å] form angles of 0 and 90° with the a_H axis and of 120 and 90° with the b_H axis, respectively. This orientation of the thermal ellipsoid indicates that the shared face between sulfur octahedra tends to remain as small as possible in order to prevent the vanadium atoms from coming too close together along the c axis. The octahedral chains seem to be a rigid unit in the structure of $BaVS_3$.

Twinning

Since the phase of $BaVS_3$ stable below the crystallographic transition has a symmetry (orthorhombic) lower than that of the initial phase (hexagonal), twin formation in the former phase has to be expected at the transition. The primitive unit cells of the hexagonal and orthorhombic phases have the same volume, which indicates that the twinning is by pseudomerohedry (Friedel, 1964) and is controlled by the hexagonal pseudosymmetry of the orthorhombic crystal lattice. The twin laws predicted by the theory are : $[001]_{60°}$, $[001]_{120°}$, $(110) \equiv [310]$, $(\bar{1}10) \equiv [3\bar{1}0]$, $(130) \equiv [110]$, $(\bar{1}30) \equiv [\bar{1}10]$, $(100) \equiv [100]$ and $(010) \equiv [010]$. These axes and mirror planes are referred to the orthorhombic cell. Since the operations of the pseudotwofold axes ($[310]$, $[3\bar{1}0]$, $[110]$, $[\bar{1}10]$, $[100]$ and $[010]$) are indistinguishable from the operations of the corresponding planes, only the latter need to be considered.

Twinning by pseudomerohedry can be easily detected as each twin law produces doubling of the spots. Fig. 2 gives a schematic representation of a precession photograph taken at 120 K with the [001] axis as the precession axis. Only the strong reflections are shown and the obliquity of all twin laws has been magnified for clarity. The twin crystal is made up of six individuals related by the laws $[001]_{60°}$, $[001]_{120°}$, (130), (100) and $(\bar{1}30)$. The lattice of one individual is outlined. In general, each spot of the hexagonal lattice splits into six orthorhombic spots. For instance, the $(\bar{3}60)$ hexagonal spot splits into six, the orthorhombic $(390)_{I}$, $(600)_{II}$, $(3\bar{9}0)_{III}$, $(\bar{3}\bar{9}0)_{IV}$, $(\bar{3}90)_{V}$ and $(600)_{VI}$ spots. The Roman numbers refer to the six different individuals. If one takes the I individual as the principal one, the II, III, IV, V and VI individuals are generated by the $[001]_{60°}$, *$[001]_{120°}$, (130), (100)* and *$(\bar{1}30)$* laws respectively. Table 3 reports the intensities of the reflections used in the orientation matrix during the intensity data collection with the Philips single-crystal diffractometer. As can be seen the transition takes place between 250 and 220 K. At room temperature and at 250 K the twelve {401} reflections have the same intensity because in the hexagonal structure they are all equivalent. The same is true for the two {004}. The slight increase in the average intensity, from 12350 to 12431 for the {401} and from 22766 to 24051 for the {004}, is due to the decrease of the thermal vibrations. At 220 K the structure has undergone the orthorhombic distortion. This can be deduced from the decrease of the intensities of the {401} and the simultaneous increase of that of the {004} reflections. The variation of the intensity of the former reflections is due to the twin formation and the misalignment with respect to each other of the various individuals forming the twin crystal. The latter reflections are not affected by the twin formation and consequently their intensity continues to increase with decreasing temperature. At the transition the twelve {401} reflections split into two independent sets of orthorhombic reflections, namely the eight {441} and the four {081}, whose intensities are not necessarily the same. At 120 K this effect is more evident than at

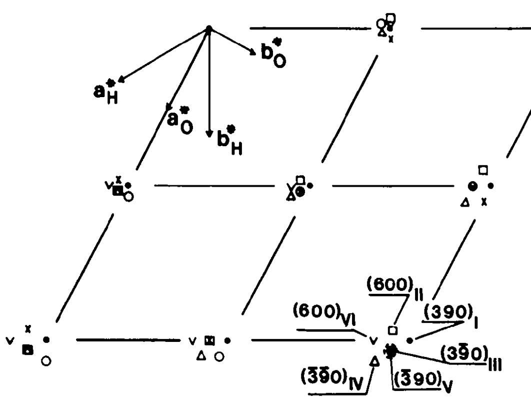

Fig. 2. Schematic representation of the precession diffraction pattern for the *ab* orthorhombic plane. Only the strong reflections are shown. The reciprocal lattice corresponding to one individual is outlined. The black dots represent the reciprocal nodes of this individual. The squares and the circles represent the nodes repeated by the two operations $[001]_{60°}$ and $[001]_{120°}$, respectively. The triangles, the crosses and the V's represent the nodes repeated by the three pseudomirror planes (130), (100) and $(\bar{1}30)$, respectively. The obliquity of all twin laws has been magnified for clarity.

Table 3. *Intensity of the reflections included in the orientation matrix in the X-ray single-crystal data collection at room and low temperatures*

Hexagonal indices	300 K	250 K	220 K	120 K	Orthorhombic indices
$4\,0\,1$	11980	12036	7482	3782	$4\,\bar{4}\,1$
$\bar{4}\,0\,\bar{1}$	11383	11699	7262	3954	$\bar{4}\,4\,\bar{1}$
$\bar{4}\,0\,1$	12597	12416	7495	3666	$\bar{4}\,4\,1$
$4\,0\,\bar{1}$	12958	12318	7515	3650	$4\,\bar{4}\,\bar{1}$
$\bar{4}\,4\,1$	12352	12698	8544	4127	$0\,8\,1$
$4\,\bar{4}\,\bar{1}$	12071	12127	8360	4159	$0\,\bar{8}\,\bar{1}$
$4\,\bar{4}\,1$	12145	12655	8345	4217	$0\,\bar{8}\,1$
$\bar{4}\,4\,\bar{1}$	11678	11877	8276	4298	$0\,8\,\bar{1}$
$0\,4\,1$	13036	12806	7439	3643	$4\,4\,1$
$0\,\bar{4}\,\bar{1}$	13185	13349	7766	3839	$\bar{4}\,\bar{4}\,\bar{1}$
$0\,4\,\bar{1}$	12458	12663	8175	3878	$4\,4\,\bar{1}$
$0\,\bar{4}\,1$	12353	12529	7934	3790	$\bar{4}\,\bar{4}\,1$
$0\,0\,4$	23484	24436	25679	27683	$0\,0\,4$
$0\,0\,\bar{4}$	22049	23666	24024	26524	$0\,0\,\bar{4}$

220 K; in fact one can readily distinguish the two independent sets, one composed of eight reflections whose average intensity is 3775 ± 120 and another of four, whose average intensity is 4200 ± 75.

The space group of the orthorhombic phase

The orthorhombic cell parameters are related to the hexagonal ones by the relation: $a_O \simeq a_H$, $b_O = \sqrt{3}a_H$ and $c_O = c_H$.

The systematic absences (*hhl* with $l = 2n + 1$) of the space group $P6_3/mmc$ are transformed to $2h,0,l$ with $l = 2n + 1$ by the transformation matrix

$$\begin{pmatrix}a\\b\\c\end{pmatrix}_O = \begin{pmatrix}1&1&0\\\bar{1}&1&0\\0&0&1\end{pmatrix}\begin{pmatrix}a\\b\\c\end{pmatrix}_H.$$

These absences, in addition to those corresponding to the *C*-centering, indicate two possible space groups for the orthorhombic phase, namely *Cmcm* and $Cmc2_1$, with four molecules per unit cell.

Actually, of the twelve equivalent hexagonal $\{hhl\}_H$ reflections four transform to the orthorhombic $\{2h,0,l\}_O$, and eight to the $\{h,3h,l\}_O$ reflections. These latter ones can have an intensity different from zero as they are of *hkl* type, for which the only systematic absence is $h + k = 2n + 1$. It is conceivable then that, with the distortion, all twelve $\{hhl\}_H$ reflections would have non-zero intensity. In this case the only space group possible would be $C222_1$, for which the systematic absences are *hkl* with $h + k = 2n + 1$ and $00l$ with $l = 2n + 1$. This space group has been suggested by Takano *et al.* (1977) as a possible one for the orthorhombic phase; however, these authors did not give any experimental evidence for their choice. Diffractometer powder diagrams, taken at 77 and 4·2 K in our laboratory, by Sayetat, Chenavas, Ghedira & Marezio (1981), did not show any peaks corresponding to reflections such as 201, 213, 412, *etc.* However, the diagrams did not show any peaks either such as 131, 132, 261, *etc.*, which corresponded to the $h,3h,l$ reflections. The precession photographs were not conclusive either as the twinning complicated their interpretation. However, they did show the systematic absence $00l$ with $l = 2n + 1$. Because of this uncertainty, in Table 4 the distortion is given for the three possible space groups, *Cmcm*, $Cmc2_1$ and $C222_1$.

Discussion

In the centrosymmetric *Cmcm* space group the vanadium atoms are in the special position 4(*a*) at (000), (00½), *etc.* The corresponding sublattice has the same orthorhombic distortion as that of the crystal lattice. Therefore, below the transition the vanadium atoms still form chains parallel to the c_O axis and they are equidistant along the chains. The barium and sulfur sublattices are more distorted than the crystal lattice as their distortion depends upon the relative positional parameters. In the non-centrosymmetric $Cmc2_1$ and $C222_1$ space groups the vanadium atoms come out of the (000) positions and the vanadium chains zig-zag along the c_O axis. In the former space group the zig-zag component is perpendicular to the a_O axis, whereas in the latter it is along the a_O axis. In both space groups the vanadium atoms are equidistant from each other along the chains, as they lie on the $z = 0$ and $z = \frac{1}{2}$ planes in the $C222_1$ space group and on the z and $z + \frac{1}{2}$ planes in $Cmc2_1$. The barium and sulfur sublattices in these non-centrosymmetric space groups have about the same distortion as the corresponding sublattices in the *Cmcm* space group. It should be pointed out that, although both the $Cmc2_1$ and $C222_1$ space groups belong to two non-centrosymmetric classes, namely *mm*2 and 222, the former allows ferroelectric and consequently piezoelectric properties, while in the latter only piezoelectricity is allowed.

A choice of the space group for the orthorhombic phase, at least between the centrosymmetric and the non-centrosymmetric ones, can be made if the large anisotropy of the thermal vibration of the vanadium atoms is interpreted in terms of a dynamical distortion of the vanadium sublattice. At room temperature the thermal ellipsoids of the vanadium atoms show an anomalously large component [0·163 (1) Å] in the *ab* basal plane with respect to the component along the *c* axis [0·106 (1) Å]. The vanadium atoms are not fixed

Table 4. *Structural arrangement of* $BaVS_3$ *at room and low temperatures*

	$P6_3/mmc$						$Cmcm$						$Cmc2_1$						$C222_1$					
V	2(*a*)	$\bar{3}m$	0	0	0		4(*a*)	2/*m*	0	0	0		4(*a*)	*m*	0	*y*	*z*	$y \simeq 0$ $z \simeq 0$	4(*a*)	2	*x*	0	0	$x \simeq 0$
Ba	2(*d*)	$\bar{6}m2$	$\frac{2}{3}$	$\frac{1}{3}$	$\frac{1}{4}$		4(*c*)	*mm*	0	*y*	$\frac{1}{4}$	$y \simeq \frac{1}{3}$	4(*a*)	*m*	0	*y*	*z*	$y \simeq \frac{1}{3}$ $z \simeq \frac{1}{4}$	4(*b*)	2	0	*y*	$\frac{1}{4}$	$y \simeq \frac{1}{3}$
S	6(*h*)	*mm*	*x*	2*x*	$\frac{1}{4}$	$x \simeq \frac{1}{6}$	4(*c*)	*mm*	0	*y*	$\frac{1}{4}$	$y \simeq \frac{5}{6}$	4(*a*)	*m*	0	*y*	*z*	$y \simeq \frac{5}{6}$ $z \simeq \frac{1}{4}$	4(*b*)	2	0	*y*	$\frac{1}{4}$	$y \simeq \frac{5}{6}$
							8(*g*)	*m*	*x*	*y*	$\frac{1}{4}$	$x \simeq \frac{1}{4}$ $y \simeq \frac{1}{12}$	8(*b*)	1	*x*	*y*	*z*	$x \simeq \frac{1}{4}$ $y \simeq \frac{1}{12}$ $z \simeq \frac{1}{4}$	8(*c*)	1	*x*	*y*	*z*	$x \simeq \frac{1}{4}$ $y \simeq \frac{1}{12}$ $z \simeq \frac{1}{4}$

on the *c* axis as the X-ray data indicate; instead they zig-zag almost perpendicularly to the c_O axis and at room temperature already form zig-zag chains. Since the vibrations of the vanadium atoms are isotropic in the basal plane, their zig-zag does not have any preferential direction in this plane. At the ~250 K transition the dynamical distortion of the vanadium sublattice becomes static and the distortion takes place only in one well defined direction.

This anisotropy drives the distortion of the other two sublattices in order to have local charge balance in the structure and the crystal symmetry becomes orthorhombic. This model of a transition from a dynamical to a static distortion is based on the assumption that the space group of the orthorhombic structure is either $Cmc2_1$ or $C222_1$, for which the vanadium positions are $(0yz)$ with $y \simeq 0$, $z \simeq 0$ and $(x00)$ with $x \simeq 0$, respectively, and consequently the centrosymmetric *Cmcm* space group can be eliminated.

The large thermal vibrations of the vanadium atoms in the hexagonal phase could also be explained by a static distortion of the vanadium sublattice in the hexagonal matrix of the other two sublattices. The distortion would not have a long-range order and the classical X-ray structure determination would yield a hexagonal arrangement for the vanadium sublattice with large thermal vibrations. However, the low *R* factor (1·1%) seems to indicate that the structure as determined from X-ray single-crystal data is not an average structure and thus the disordered static model can be rejected.

References

CROMER, D. T. & LIBERMAN, D. (1970). *J. Chem. Phys.* **53**, 1891–1898.

CROMER, D. T. & WABER, J. T. (1965). *Acta Cryst.* **18**, 104–109.

FRIEDEL, G. (1964). *Leçons de Cristallographie.* Paris: Blanchard.

GARDNER, R. A., VLASSE, M. & WOLD, A. (1969). *Acta Cryst.* B**25**, 781–787.

MASSENET, O., BUDER, R., SINCE, J. J., SCHLENKER, C., MERCIER, J., KELBER, J. & STUCKY, D. G. (1978). *Mater. Res. Bull.* **13**, 187–195.

MASSENET, O., SINCE, J. J., MERCIER, J., AVIGNON, M., BUDER, R., NGUYEN, V. D. & KELBER, J. (1979). *J. Phys. Chem. Solids*, **40**, 573–577.

SAYETAT, F., CHENAVAS, J., GHEDIRA, M. & MAREZIO, M. (1981). In the press.

TAKANO, M., KOSUGI, H., NAKANISHI, N., SHIMADA, M., WADA, T. & KOIZUMI, M. (1977). *J. Phys. Soc. Jpn*, **43**, 1101–1102.

Acta Cryst. (1981). B**37**, 1496–1500

The Structure of Synthetic Andersonite, $Na_2Ca[UO_2(CO_3)_3].xH_2O$ ($x \simeq 5{\cdot}6$)

BY ALESSANDRO CODA,* ANTONIO DELLA GIUSTA† AND VITTORIO TAZZOLI

Centro di Studio per la Cristallografia Strutturale del Consiglio Nazionale delle Ricerche, Istituto di Mineralogia dell'Università, Via Bassi 4, 27100 *Pavia, Italy*

(*Received* 30 *January* 1980; *accepted* 2 *February* 1981)

Abstract

$Na_2Ca[UO_2(CO_3)_3].xH_2O$ ($x \simeq 5{\cdot}6$), $M_r = 644$, is trigonal, $R\bar{3}m$, $a = 17{\cdot}902$ (4), $c = 23{\cdot}734$ (4) Å, $Z = 18$, $D_m = 2{\cdot}8$, $D_c = 2{\cdot}86$ Mg m^{-3}, $F(000) = 5400$, $T = 295$ K. It is found as the mineral andersonite. The structure was solved by use of a synthetic sample, and refined anisotropically to $R_w = 4{\cdot}9\%$ by full-matrix least-squares methods based on 794 independent counter reflections. The coordination polyhedron of U is a hexagonal bipyramid with two apical O atoms much closer to U than the others [1·81 (2) and 1·78 (2) Å, angle 180 (1)°], and six equatorial O atoms belonging to three bidentate CO_3^{2-} anions. Two independent Na atoms and one Ca have coordination numbers 6, 6 and 7 respectively. Only five water molecules in the formula were found in the final Fourier map; the possible statistical distribution of the remainder in a structure channel is discussed.

Introduction

Andersonite is a rare uranyl carbonate (tricarbonatodioxouranate) found in the Hillside mine, Yavapai

---

* Permanent address: Istituto di Cristallografia dell'Università, Viale Taramelli 16, 27100 Pavia, Italy.

† Permanent address: Istituto di Mineralogia dell'Università, Palazzo delle Scienze, Corso Europa, 16132 Genova, Italy.

0567-7408/81/081496-05$01.00